Mechanical properties of composite timber flitch beams laminated vertically with fibre reinforced plastic and steel reinforcements

Parvez ALAM
Ph.D. Student
University of Bath
Bath, UK.

B.Eng. (Hons.), GIMMM. Student member of the Institute of Wood Science. Currently in final year of PhD studies at University of Bath, England. Born 11.8.75 in Dorset, UK. Married to Catharina with two children, Lilja (2½) and Shujon (1).

Martin. P. ANSELL
Senior Lecturer
University of Bath
Bath, UK.

BSc, PhD, FIMMM, FIWSc. President of UK Institute of Wood Science from 1994 to 1996. Research interests also include fatigue of timber and development of natural fibre composites

Dave SMEDLEY
Technical Director
Rotafix Ltd.
Abercraf, Swansea, UK.

Trained as a surface coating chemist. Developed and patented zinc phosphate as an anti corrosive, environmentally safe substitute for red lead. Has worked internationally on developing epoxy road surface joints. Currently specialises with industrial adhesives.

Summary

Composite timber beams have been manufactured in two different geometric configurations bonding in secondary adherends such as steel and fibre reinforced plastic plates (FRP) to vertically reinforce Kerto S laminated veneer lumber (LVL), a primary adherend. The geometric configuration of the reinforcement was found to affect the extent of improvement in flexural strength compared with the un-reinforced LVL beams. The modes of failure and the flexural moduli were found to be influenced by the reinforcing material and its properties.

Keywords: Flitch-beam, Timber, FRP, Steel, Reinforced, LVL, Finite-Element-Analysis

1. Introduction

Flitch reinforcements lie vertically inside timber sections and are used to enhance the mechanical performance of timber beams. Previous studies have highlighted the merits of nailed steel flitch beams and have evaluated the extent of improvement in the mechanical properties of beams in flexure [1] and the significance of intimate connection between composite members [2] and [3]. Stern and Kumar [1] have reported that flitch beams in flexure rose in strength and stiffness by 45% and 48% respectively as a result of vertically laminating two steel plates between 3 timber members. Alam and Ansell [3] have reported that decreasing modulus of rupture and increasing modulus of elasticity is a function of increasing nailing density.

Very little has been reported on flitch reinforcements using FRP plates. The majority of studies have considered horizontal laminations of the tensile face. Johns and Lacroix [4] studied timber beams laminated both vertically and horizontally by U- shaped glass fibre reinforced plastic. These beams were reported to give up to a 90% increase in flexural strength. Chajes *et al* [5] recorded a stiffness increase of 21% with a horizontal tensile face lamination of carbon fibre reinforced plastic being 0.67% of the depth of the whole beam.

The present paper aims to present and compare the mechanical properties and the failure modes of LVL composite beams laminated vertically in two alternate configurations with steel and FRP plates. The modified steel and FRP flitch beams are manufactured using a bonded method rather than the more traditional bolted assembly

2. Sample configurations and experimental methods

2.1 Samples

Grade 43 mild steel, glass fibre reinforced plastic (GFRP), three layers of glass fibre reinforced polyurethane (FULCRUM) and carbon fibre reinforced plastic (CFRP) were used as vertically laminating reinforcements for LVL (1900mm long, 110mm deep and 51mm wide). Two test configurations were used and designated phase1 and phase 2. Phase 1 composites comprised full depth plate reinforcement laminated between two LVL sections. Phase 2 composites were constructed by adhering two LVL sections, routing grooves 40mm deep at the top and bottom faces of the beam and slotting adhesively bonded 40mm plate reinforcement into the grooves.

Composite elements were glued together using CB10TSS adhesive, a low modulus thick film epoxy adhesive. The reinforcing elements were subjected to different surface treatments prior to gluing. Steel plates were grit blasted immediately before gluing, CFRP plates were covered by a 'peel ply' layer which was removed prior to gluing, the GFRP surface was abraded using a miniature grit blasting machine with sodium carbonate abrasive and the FULCRUM was left untreated as it has an inherently rough surface. The cross sectional layout for phase 1 and 2 beams is shown in Figure 1.

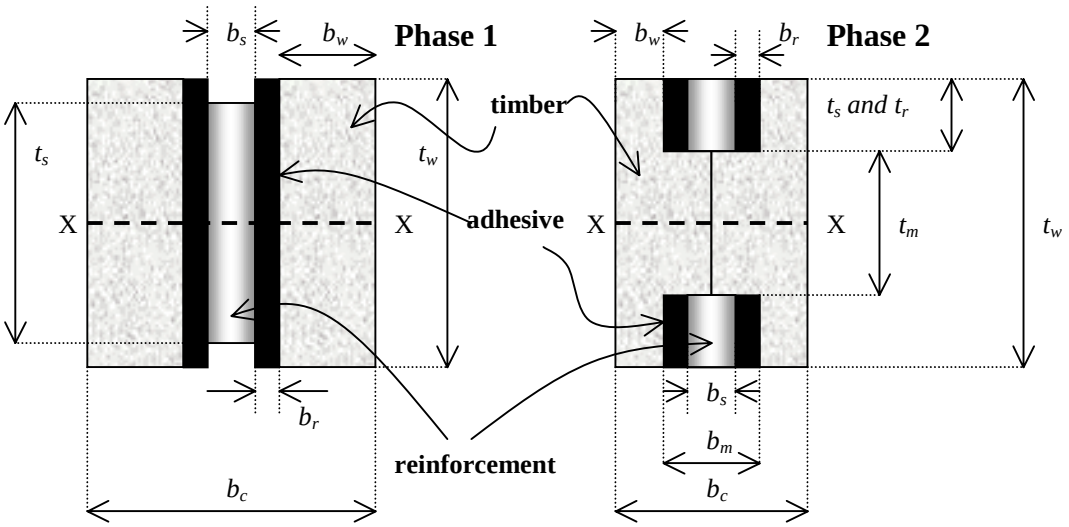

Figure 1. Cross sectional layout of composite elements for phase 1 and 2 beams. The notations; b and t refer to the width and the depth respectively. The subscripts; $_{w, s, r, m}$ and $_c$ refer to wood, reinforcement, adhesive, width of routed grooves and the whole composite respectively.

Equations (1) and (2) describe the transformed section properties for phase 1 composites about the line x-x. Transformed section properties about the line x-x are expressed for phase 2 composites by equations (3) and (4). I_t is the transformed second moment of area, W_t is the transformed section modulus and E is the elastic modulus. The dimensions of the reinforcements are listed in Table 1.

$$I_t = \frac{b_w t_w^3}{6} + \frac{E_s b_s t_s^3}{E_w 12} + \frac{E_r b_r t_r^3}{E_w 6} \tag{1}$$

$$W_t = \frac{2I_t}{t_w} \tag{2}$$

$$I_t = \left\{ 0.125 b_w t_w^3 + 4\left(\frac{E_r}{E_w}\right)(b_r t_r)(t_m + 0.5t_r)^2 + 0.5 b_m t_m^3 + 2\left(\frac{E_s}{E_w}\right)(b_s t_s)(t_m + 0.5t_s)^2 \right\} + \left\{ 0.125\left(\frac{b_w t_w^3}{3}\right) + \left(\frac{E_r}{E_w}\right)\left(\frac{b_r t_r^3}{3}\right)\frac{b_m t_m^3}{6} + \left(\frac{E_s}{E_w}\right)\left(\frac{b_s t_s^3}{6}\right) \right\} \tag{3}$$

$$W_t = \frac{2I_t}{t_w} \tag{4}$$

Table 1. Dimensions of the reinforcing laminates.

	Phase 1			Phase 2		
	Length /mm	**Depth of reinforcement /mm**	**Thickness /mm**	**Length /mm**	**Depth of reinforcement /mm**	**Thickness /mm**
STEEL	1900	100	6.0	1900	40 × 2	5.0
CFRP	1900	100	1.5	1900	40 × 2	1.5
GFRP	1900	100	4.0	1900	40 × 2	4.0
FULCRUM	1900	100	1.2 × 3	1900	40 × 2	1.2 × 3

2.2 Experimental

Testing was conducted according to BS EN 408:1995. Composite beams were subjected to four-point bending at a crosshead rate of 2mm.min^{-1}. A total of three beams were tested for each reinforcement type in each phase. A linear variable differential transformer (LVDT) displacement transducer was located between the central rollers and used to measure the centre point deflection. Strain gauges were attached to a single beam from each phase. Figure 2 shows the roller positions. The general positions of the strain gauges relative to the LVDT are shown in Figure 3.

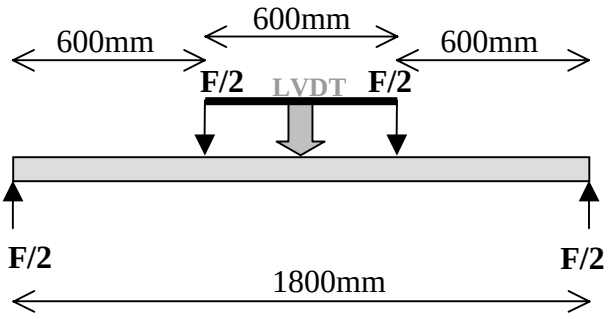

Figure 2. Four-point bending test arrangement in accordance with BS EN 408:1995.

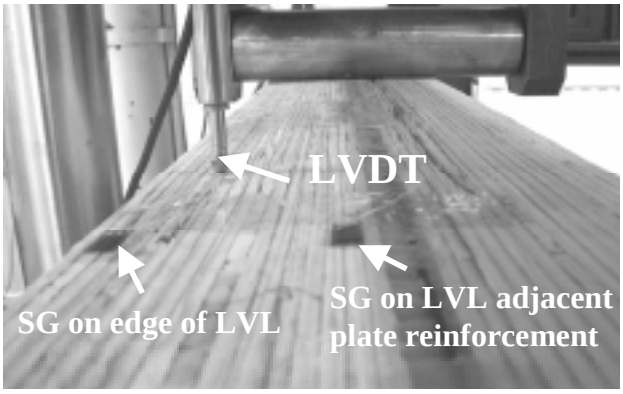

Figure 3. Positions of strain gauges and LVDT on the upper face of the composite beams.

3. Results and Discussion

3.1 Mechanical properties

Median values for flexural strength, σ_f, were taken from each group and the percentage deviation, đ, from un-reinforced LVL beams was calculated, Table 2. The transformed section properties were used to calculate σ_f, which is represented by the equation $[aF_{max}]/[2W_t]$ where a is the distance between the loading position and the nearest support and F_{max} is the maximum load experienced by the composite. The phase 2 beams all showed an increase in σ_f relative to un-reinforced LVL whereas the majority of phase 1 beams did not. In phase 2, CFRP-LVL beams exhibit σ_f values superior to those of steel reinforced beams, the σ_f values for FULCRUM-LVL beams are equivalent to that of steel and GFRP-LVL composites have the lowest σ_f values. This suggests that it is more effective to situate reinforcement material at the upper and lower faces of the beams, than to have full depth reinforcement.

Figures 4 and 5 show stress-strain plots for one beam from each group for phase 1 and 2 beams respectively. The stress is calculated using an average composite section modulus and not W_t. This allows the differences in flexural moduli, E_f, to be identified. The strain is taken from the strain gauges, which are less sensitive than the LVDT to global movement in the beam and are fitted to only measure strains along the longitudinal beam axis.

Table 2. Strength, % deviations and stiffness properties of composite beams (median values).

	Phase 1			Phase 2		
	σ_f/MPa	đ/%	E_f/GPa	σ_f/MPa	đ/%	E_f/GPa
STEEL-LVL	47.3	-16.0	37.1	67.9	+20.1	29.9
CFRP-LVL	64.0	+13.4	22.6	71.0	+25.8	18.9
GFRP-LVL	51.6	-0.9	18.8	67.8	+15.8	16.4
FULCRUM-LVL	55.9	-8.6	16.6	65.4	+20.1	16.9

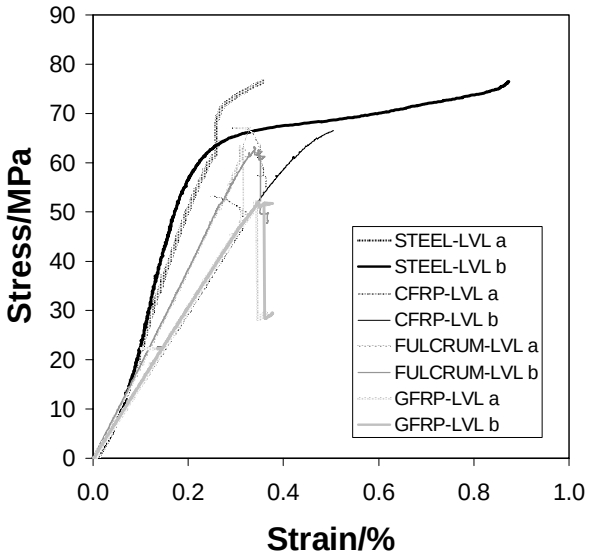

Figure 4. Stress-strain plot for Phase 1 beams

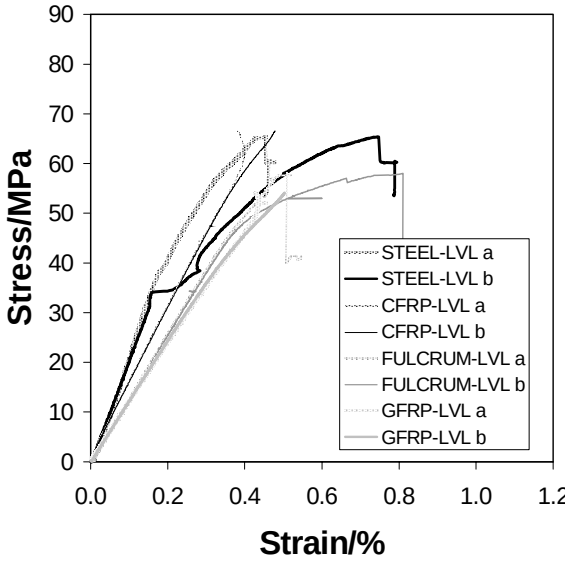

Figure 5. Stress-strain plot for Phase 2 beams

Strain gauges adjacent to the reinforcement and on the edge of the LVL are labelled 'a' and 'b' respectively.

E_f is a function of the elastic modulus of the laminating material. Higher modulus reinforcing materials generally result in superior E_f. Steel-LVL composites exhibit the greatest ductility, while the FRP-LVL composites tend to be more brittle. In every case, the failure strain on the edge of the LVL is higher than the strain closer to the centre where the reinforcement is positioned. It is plausible to suggest that the reinforcement constrains failure in the adjacent LVL more effectively as a function of decreasing distance from the reinforcement.

The yield strain, ε_y, of the reinforcing elements is paramount to the failure mechanism of the composite. Tests have shown that the ε_y of LVL is between 0.3-0.4% and ε_y for steel is 0.15%. ε_y for CFRP is 0.75% and ε_y for GFRP is 2.5% [6].

Although ε_y for steel is lower than LVL; the process of strain hardening, the intimacy of contact between composite elements and the inherently ductile nature of mild steel allows the LVL in close proximity to he steel to fail at higher strains than it would if un-reinforced. Brittle failure can be anticipated for FRP-LVL composites due to the higher ε_y of the FRP plate reinforcements compared with LVL and the brittle nature of FRP failure. This can be seen in every case except phase 2 FULCRUM where the LVL closest to the FULCRUM exhibits brittle behaviour while the LVL at the edge is less so.

3.2 Failure modes and observations

Both phase 1 and 2 steel-LVL composites experienced compressive failure, Figure 6, which is possibly a consequence of the lower ε_y of mild steel relative to LVL. This was followed by catastrophic fracture on the tensile face of the LVL, Figure 7. Steel-adhesive de-bonding was noted for only phase 2 beams, Figure 8.

All composite beams experienced catastrophic fracture on the tensile face. Unlike the phase 2 steel-LVL composite beams, CFRP and FULCRUM reinforcements did not separate from the adhesive. The phase 2 CFRP however did de-bond and de-laminate. Phase 2 FRP-LVL beams showed evidence of compressive buckling in the LVL. However, no indication of compressive failure was determined from a visual inspection of phase 1 beams.

Figure 6. An example of compressive failure in a steel-LVL composite beam.

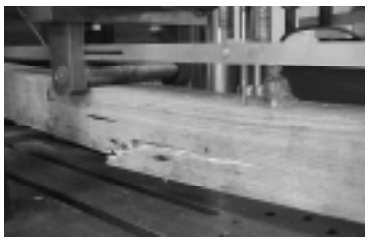

Figure 7. Tensile fracture in a steel-LVL composite beam.

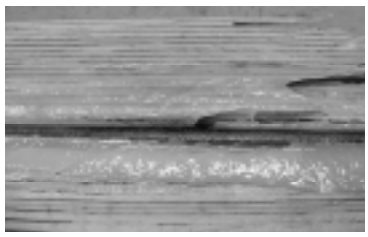

Figure 8. De-bonding between adhesive and steel leading to interfacial slip.

A close examination of a sawn cross section from each phase of CFRP and FULCRUM reinforced beams clearly illustrates that on the tensile edge, tangential cracks preferentially propagate through the LVL adjacent to the reinforcement, as opposed to traversing into the adhesive, Figures 9-12. The GFRP laminates in both phase 1 and 2 did experience de-bonding from the adhesive, in contrast to the other FRP types. The de-bond from the GFRP leads to tangential fracture in the adhesive, which in turn leads to fracture in the LVL, Figures 13 and 14. Whether the crack path initiates or ends at the de-bond is indefinite.

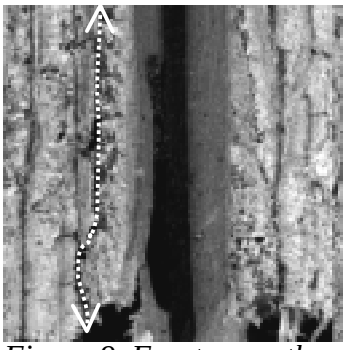

Figure 9. Fracture path near CFRP laminate, Phase 1.

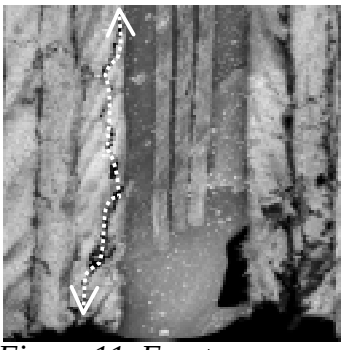

Figure 11. Fracture near FULCRUM laminate, Phase 1.

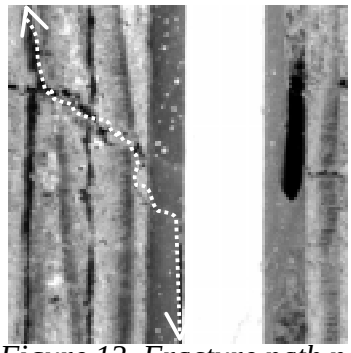

Figure 13. Fracture path near GFRP laminate, Phase 1.

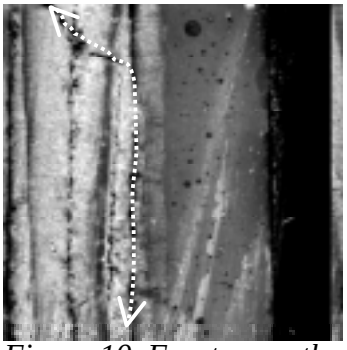

Figure 10. Fracture path near CFRP laminate, Phase 2.

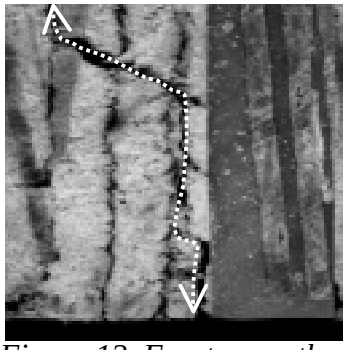

Figure 12. Fracture path near FULCRUM laminate, Phase 2.

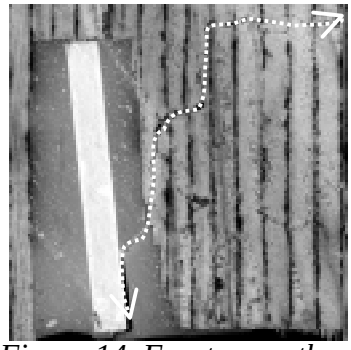

Figure 14. Fracture path near GFRP laminate, Phase 2.

3.3 Comparison of geometric arrangement using finite element analysis

Finite element models were developed to illustrate the effect on the distribution of perpendicular-to-axis shear stresses, (yz), for phase 1 and phase 2 beam configurations. Figures 14 and 15 show a segment from the centre of phase 1 and 2 steel-LVL beams respectively. In both cases, the shear stresses are highest near the reinforcements where the majority of stress transfer occurs on loading. The stresses then diminish towards the edge of the LVL. Shear stresses are concentrated to the upper and lower faces of the phase 2 beam segment. The phase 1 beam segment however, experiences a shear stress distribution throughout the depth of the LVL as a consequence of having a full depth plate.

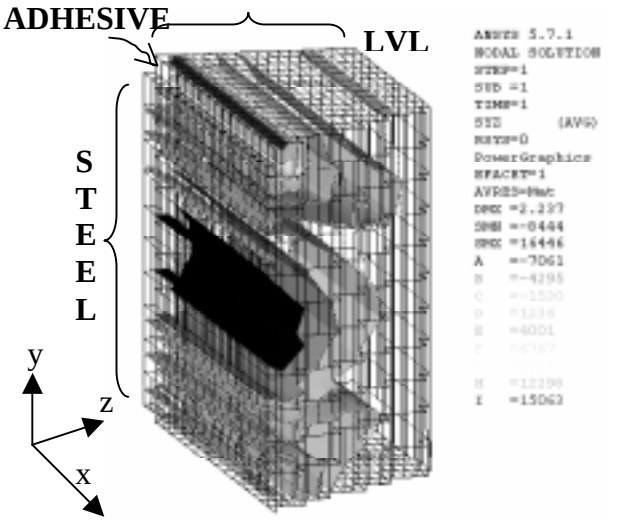

Figure 14. Shear stress contours in a section of a phase 1 steel-LVL beam.

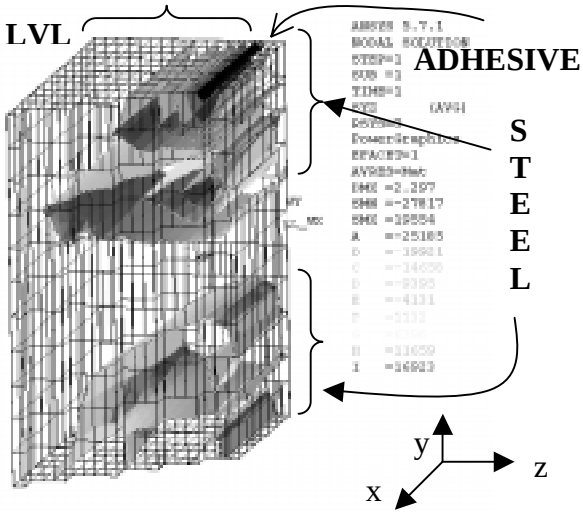

Figure 15. Shear stress contours in a section of a phase 2 steel-LVL beam.

4. Conclusions

Using the transformed section approach to analyse the composite configurations demonstrates that vertically laminating the upper and lower faces of LVL in flexion is more effective as a means of improving σ_f than having a full depth vertical lamination. The E_f of a composite beam is dependant upon the elastic modulus of the reinforcing material. Materials with a higher elastic modulus will yield higher E_f values for the composite. Failure modes have been described for steel-LVL composite beams and LVL beams reinforced with various FRP plates. Fracture paths have been identified and illustrated in the vicinity of the plate reinforcements for the FRP-LVL composites.

In phase 1, the configuration is more appropriate to upgrading a section size and length within the confines of a workshop where a sandwich and laminating technique can be used. Phase 2, which has been compared with directly in performance, is designed for installation in-situ into timber using appropriate portable tools. This enables the minimal intervention to the individual timber component within the building, while affording the maximum upgrading of the timber combined with the least aesthetically displeasing effect.

5. Acknowledgements

The authors thank the EPSRC for their support and Stan Bowen for his indispensable help.

6. References

[1] Stern, E. G. and Kumar, V. K., “Flitch Beams”, *Forest Products Journal*, Vol. 23, No. 5, 1973, pp. 40-47.

[2] Coleman, G. E. and Hurst, H. T., “Timber Structures Reinforced with Light Gage Steel”, *Forest Products Journal*, Vol. 24, No. 7, 1974, pp. 45-53.

[3] Alam, P. and Ansell, M. P., “Development of a Finite Element Model to Predict the Flexural Response of Steel-LVL Composite Beams Connected by Fired Nails and Subjected to Static Bending Loads”, *Second International Conference of the European Society for Wood Mechanics, Stockholm, Sweden*, 2003.

[4] Johns, K. C. and Lacroix, S., “Composite Reinforcement of Timber in Bending”, *Canadian Journal of Civil Engineering*, Vol. 27, 2000, pp. 899-906.

[5] Chajes, M. J., Kaliakin, V. N. and Holsinger, S. D., “Experimental Testing of Composite Wood Beams for Use in Timber Brides”, *Proceedings of the Fourth International Bridge Engineering Conference*, Vol. 2, 1995, pp. 371-380.

[6] Plevris, N. and Triantafillou, T. C., “FRP-Reinforced Wood as Structural Material”, *ASCE Journal of Materials in Civil Engineering*, Vol. 3, No. 3, 1992, pp. 300-317.